Positron and positronium in Al_2O_3 nanopowders

Cite as: AIP Conference Proceedings **2182**, 050008 (2019); https://doi.org/10.1063/1.5135851
Published Online: 27 December 2019

P. S. Stepanov, F. A. Selim, S. V. Stepanov, and V. M. Byakov

Positron and Positronium in Al_2O_3 nanopowders

P.S. Stepanov[1,a)], F.A. Selim[1], S.V. Stepanov[2,3] and V.M. Byakov[2,3,4]

[1]*Center for Photochemical Sciences, Department of Physics and Astronomy, Bowling Green State University, OH 43403 USA*
[2]*NRC "Kurchatov Institute" – Institute for Theoretical and Experimental Physics, 117218, Moscow, Russia*
[3]*Institute for Theoretical and Experimental Physics named by A.I. Alikhanov of National Research Centre "Kurchatov Institute", Moscow, 117218 Russia*
[4]*D. Mendeleyev University of Chemical Technology of Russia, Miusskaya sq., 9, 125047, Moscow, Russia*

[a)]Corresponding author: petrs@bgsu.edu

Abstract. Software that allows fitting positron lifetime (LT) and coincidence Doppler broadened (CDB) positron annihilation spectra of nanodispersed dielectric powders is developed. Computer program takes into account following effects: possibility of e^+ trapping by vacancy-type defects, formation of the surface-bound e^+ states, formation and thermalization of Ps atoms in intergranular space. In order to test the developed software, lifetime and coincident Doppler broadened spectra of Al_2O_3 nanopowders with different grain sizes are acquired. Suggested physical model of the processes involved gives self-consistent interpretation of the spectra. Parameters of the thermalization kinetics of Ps and its ortho-para conversion due to presence of O_2 molecules adsorbed on the crystallite surface are obtained.

INTRODUCTION AND FORMULATION OF THE MODEL

There are several projects carried out by F.A. Selim research group (BGSU, Ohio) aimed on manufacturing and investigations of transparent ceramics and nanophosphors (YAG garnets, ceramics doped with rear-earth ions, ZnO), which have wide applications in optical devices and electronics. Usually ceramics are grown by means of sintering of nanopowders of different oxides (Y_2O_3, Al_2O_3, SiO_2) with some additives [1]. Structural vacancy-type defects, defects raised after implantation of dopants as well as sorption of molecular oxygen from air strongly affect on transparency, light scattering and mechanical properties of the produced samples. Therefore, monitoring defects and impurities on each stage of the sample manufacturing is an important problem. In order to investigate it we utilize positron annihilation lifetime spectroscopy (PALS) and coincidence Doppler broadening spectroscopy (CDB) [3, 5].

We propose and apply a certain physical model that accounts on the behaviour of positrons and positronium atoms in oxide nanopowders. A series of LT and CDB measurements of Al_2O_3 nanopowders of a different grain size (50, 300 nm and 1 and 3 μm) are carried out to proove the vlitity of the proposed model.

In the first iteration we utilize simplifed version of the model [3] where we assume that positron instantly reaches crystallite boundary ($\lambda_J \to \infty$, $\lambda_{\rm Ps} \to 0$). In this case Ps atom can only be formed in between of the grains and $n_{\rm Ps}(t)$ disappears from the initial set of equations:

$$n_b(t) = (1-P_{\rm Ps})e^{-(\lambda_b+\varkappa_v+\varkappa_s)t}, \tag{1}$$

$$n_v(t) = (1-P_{\rm Ps})\frac{\varkappa_v[e^{-\lambda_v t}-e^{-(\lambda_b+\varkappa_v+\varkappa_s)t}]}{\lambda_b+\varkappa_v+\varkappa_s-\lambda_v}, \tag{2}$$

$$n_s(t) = (1-P_{\rm Ps})\frac{\varkappa_s[e^{-\lambda_s t}-e^{-(\lambda_b+\varkappa_v+\varkappa_s)t}]}{\lambda_b+\varkappa_v+\varkappa_s-\lambda_s}, \tag{3}$$

$$n_o(t) = \frac{3P_{\rm Ps}}{4}\cdot\exp\left(-\int_0^t\frac{\lambda_{opc}(\tau)}{4}d\tau\right), \tag{4}$$

$$\dot{n}_p(t) = \frac{\lambda_{opc}(t)}{4}n_o-\lambda_{2\gamma}n_p\,, \qquad n_p(0)=\frac{P_{\rm Ps}}{4}. \tag{5}$$

The 18th International Conference on Positron Annihilation (ICPA-18)
AIP Conf. Proc. 2182, 050008-1–050008-5; https://doi.org/10.1063/1.5135851
Published by AIP Publishing. 978-0-7354-1929-2/$30.00

Here $n_b(t)$, $n_v(t)$ and $n_s(t)$ are probabilities of observing a positron at a time moment t in following states, respectively: 1) quasi-free positron (qf-e^+) in the **bulk** of Al_2O_3 crystallite that annihilates with a rate λ_b; 2) e^+ trapped in Al vacancy (vac-e^+) with annihilation rate λ_v; 3) e^+ localized in a bound state on the crystallite surface (surf-e^+), annihilates with a rate λ_s.

Trapping rates of the qf-e^+ captured into the Al-vacancies and into surface bound states at the crystalline border are denoted by values $\varkappa_v$ and $\varkappa_s$.

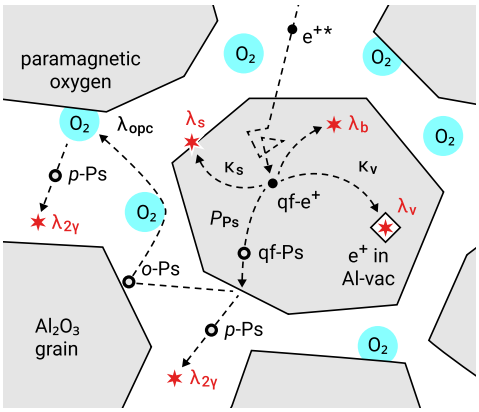

FIGURE 1. Understanding the parameters of the simplified model of positron and positronium in aluminum oxide nanopowders.

First three Eqs. (1-3) describe behavior of a qf-e^+ that escaped formation of a positronium (Ps) atom. These equations correspond to processes of annihilation of qf-e^+ in the bulk of crystallites, as well as their trapping by vacancies and transformation into surface-bound states. These expressions should be familiar to the reader because they are inherited from the Standard Trapping Model equations [4].

Probability of Ps atom formation in between of the crystallites is denoted by $P_{\rm Ps}$. Functions $n_o(t)$ and $n_p(t)$ stand for probabilities of observing ortho- and para-positronium (o-Ps, p-Ps) at a moment of time t.

Usually an interaction of Ps with oxygen molecules (as well as some other molecules possessing oxidizing properties, like Cl_2, Br_2, I_2) is more important than with other neutral molecules, for example with nitrogen. In most cases interaction with O_2 leads to the Ps spin conversion and/or oxidation. Pick-off annihilation of Ps, which arises from so to say "elastic" collisions with gas molecules (N_2) or surface of crystallites, is usually less important, because time of these collisions is very short. One may say that interaction with oxygen molecules resembles a "sticky" collision (unstable complex formation), but not the elastic one. Therefore, below we restrict ourselves to the simplest case - accounting for the Ps interaction with O_2, which leads to Ps ortho-para conversion ($\lambda_{opc}(t)$ is the rate of this process, it depends on Ps velocity [2]). Later on we plan to take into account other possible contributions to annihilation of o-Ps (including its 3γ-annihilation, $\lambda_{3\gamma} = 0.007$ ns^{-1}).

Expression for the ortho-para conversion rate of the Ps atom is given in [3]:

$$\lambda_{opc}(t) = \frac{\mu v_{th}}{\ell} \cdot \frac{1 + \nu e^{-\alpha t}}{1 - \nu e^{-\alpha t}}, \qquad \nu = \frac{v_0 - v_{th}}{v_0 + v_{th}}, \qquad \alpha = \frac{2mv_{th}}{M\ell}. \tag{6}$$

Here v_0 is the initial Ps velocity at the moment when qf-Ps escapes from the crystallite into intercrystallite space; $v_{th} \approx 8 \cdot 10^6$ cm/s is the velocity of Ps at room temperature. Mass of a Ps atom is expressed by m whereas M is the mass of a crystallite volume that accepts the recoil energy colliding with Ps. Variable ℓ is the characteristic distance between the crystallites.

Substituting $\lambda_{opc}(t)$ into equation (4) for $n_o(t)$, we observe that kinetics of o-Ps annihilation has a non-exponential character:

$$n_o(t) = \frac{3P_{\rm Ps}}{4} \exp\left(-\frac{\mu v_{th} t}{4\ell} - \frac{\mu M}{4m} \ln \frac{1 - \nu e^{-\alpha t}}{1 - \nu}\right). \tag{7}$$

Annihilation kinetics of the p-Ps can be obtained by solving equation (5). We take into account that the 2γ annihilation rate of a p-Ps atom ($\lambda_{2\gamma} = 8$ ns^{-1}) is significantly larger compared to all other annihilation rates:

$$n_p(t) \approx \frac{P_{\rm Ps}}{4} e^{-\lambda_{2\gamma} t} + \int_0^t \frac{\lambda_{opc}(\tau) n_o(\tau)}{4} e^{-\lambda_{2\gamma}(t-\tau)} d\tau \approx \frac{P_{\rm Ps}}{4} e^{-\lambda_{2\gamma} t} + \frac{\lambda_{opc}(t)}{4\lambda_{2\gamma}} n_o(t). \tag{8}$$

In order to estimate the value of this integral, we used the fact that the function $f(\tau > t) = 0$, $f(\tau < t) = \lambda_{2\gamma} e^{-\lambda_{2\gamma}(t-\tau)}$ at large $\lambda_{2\gamma}$ behaves like a δ-function. The first term in (8) describes annihilation of p-Ps, which was formed directly when e^+e^- pair entered the intercrystallite space; the second term is annihilation of p-Ps, formed via ortho-para conversion mechanism.

Now, we can calculate the shape of the LT spectrum:

$$C_{2\gamma}(t) \propto \lambda_b n_b + \lambda_v n_v + \lambda_s n_s + \lambda_{2\gamma} n_p = \lambda_b n_b + \lambda_v n_v + \lambda_s n_s + \frac{\lambda_{2\gamma} P_{\rm Ps}}{4} e^{-\lambda_{2\gamma} t} + \frac{\lambda_{opc}(t)}{4} n_o(t). \tag{9}$$

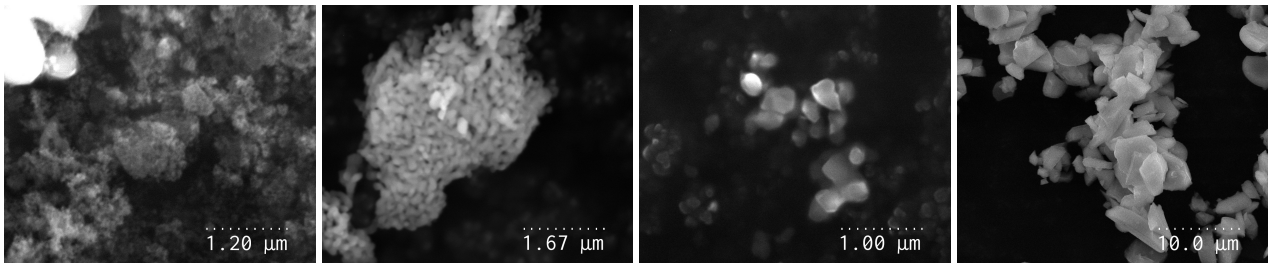

FIGURE 2. SEM imagies of the investigated Al_2O_3 powders (left to right: 50 nm, 300 nm, 1 μm and 3μm).

The integral of the last term, which is needed to speed up the numerical calculations, can be easily taken:

$$\int_0^t \frac{\lambda_{opc}(\tau)}{4} n_o(\tau) d\tau = \frac{3P_{\rm Ps}}{4}\left(1 - e^{-I(t)}\right), \qquad I(t) = \int_0^t \lambda_{opc}(\tau) d\tau = \frac{\mu v_{th} t}{4\ell} + \frac{\mu M}{4m} \ln \frac{1 - \nu e^{-\alpha t}}{1 - \nu}.$$

DATA ACQUISITION AND PROCESSING

A digital CDB spctrometer with a pair or HPGe detectors (energy resolution 1 keV) manipulated by two Canberra LYNX analyzers working in a Timestamp Mode [5] was used to acquire CDB spectra of the studied powders. Conventional lifetime spectrometer built of ORTEC components with two H3177 phototubes equipped with BaF_2 scintillation crystals (energy resolution of 370ps) was used to acquire the LT spectra. Some Al_2O_3 sample spectra were acquired at a different Time to Amplitude Converter (TAC) ranges.

We start spectra analysis by fitting CDB spectra with a set of gaussian components corresponding to e^+ annihilation with electrons of a different energies. The component of the CDB spectrum with the smallest FWHM of about 0.1 keV corresponds to the self-annihilation of the p-Ps atoms (see figure 3).

Since the qf-Ps state is excluded from the consideration in our model, the intensity of the narrow component is equal to the Ps formation probability: $Y_p = P_{\rm Ps}$. Therefore the fitting of LT spectra was carried out with the value of $P_{\rm Ps}$ set to Y_p.

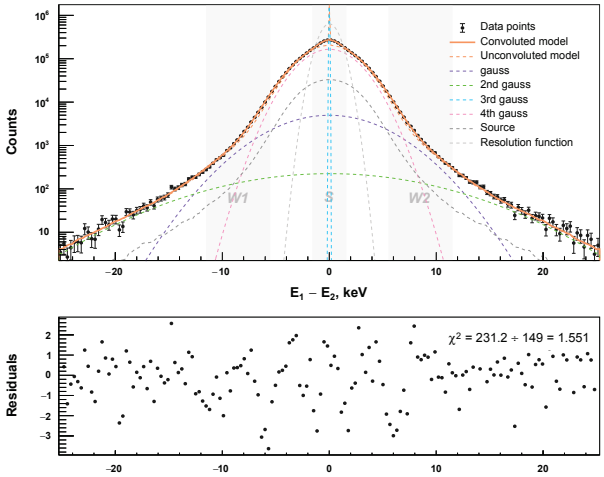

FIGURE 3. CDB spectrum of a Al_2O_3 powder (50 nm powder size) deconvoluted into gaussian components. The most narrow component (3rd gauss) corresponds to annihilation of the p-Ps atoms.

The calculations of the characteristic distance ℓ between the crystallites for each studied sample are derived from the powder density measurements. We use trivial relationship $(1 + \ell/2R)^3 = \rho_{cryst}/\rho_{powder}$, where $2R$ is an average diameter of the crystallite, $\rho_{cryst} \simeq 4$ g/cm^3 is the density of the crystalline Al_2O_3 and ρ_{powder} is its measured macroscopic density.

Diameter of the crystallites is calculated from the SEM images of the studied powders (see figure 2) with the help of the ImageJ software. Following diameter values are estimated: 60±40 nm (50 nm powder), 170±110 nm (300 nm powder), 0.28±0.23 μm (1 μm powder) and 3.5±2.7 μm (3 μm powder). The densities of the correspondent samples (ρ_{powder}) are measured as following: 0.45 g/cm^3, 0.65 (300 nm), 0.85 (1μm) and 2.0 (3 μm).

When processing the LT spectra it is important to calculate and the value of random coincidence background in advance and fix it during the subsequent fit. This value is obtained from fitting only the left part of the spectrum (to the left of the annihilation peak). This provides correct parameter values for the larger-lifetime range of the LT spectra;

TABLE 1. Results of fitting of LT and CDB spectra of Al_2O_3 powders.

γ-Al_2O_3 ⌀ 50 nm	**TAC range**	**Total counts**	**Model**	τ_1 I_1	τ_2 I_2	τ_3 I_3
	50 ns	3.6 M (35cps)	3-exp	0.23 ns 63%	0.5 ns 28%	24 ns 8%
	100 ns	1.2 M (7 cps)	3-exp	0.25 ns 73%	0.62 ns 16%	46 ns 11%
	200 ns	2.8 M (2 cps)	3-exp	0.26 ns 75%	0.67ns 12%	59 ns 13%
	Trapping model with thermalization τ_{bulk} = 0.18 ns (fixed)			τ_v = 0.25 ns κ_v = 18 ns^{-1}	τ_s = 0.47 ns κ_s = 6 ns^{-1}	P_{Ps} = **14.6%**, l = 60 nm $\mu = 1.2 \cdot 10^{-5}$, $m/M = 2 \cdot 10^{-6}$
	CDB gaussians (FWHMs, intensities)			4±1 meV, **14.6 %**	15 eV, 80%	56 eV, 5% 217 eV, 0.4%
α-Al_2O_3 ⌀ 300 nm	**TAC range**	**Total counts**	**Model**	τ_1 I_1	τ_2 I_2	τ_3 I_3
	50 ns	3.3 M	3-exp	0.21 ns 43 %	0.43 ns 54 %	23 ns 3 %
	100 ns	1.1 M	3-exp	0.28 ns 66 %	0.50 ns 29 %	40 ns 5 %
	Trapping model with thermalization τ_{bulk} = 0.18 ns (fixed)			τ_v = 0.26 ns κ_v = 10 ns^{-1}	τ_s = 0.46 ns κ_s = 8 ns^{-1}	P_{Ps} = **4.3 %**, l = 140 nm $\mu = 4 \cdot 10^{-5}$, $m/M = 2 \cdot 10^{-6}$
	CDB gaussians (FWHMs, intensities)			4±6 meV, **4.3%**	15 eV, 90%	57 eV, 5% 236 eV, 0.4 %
α-Al_2O_3 ⌀ 1 μm	**TAC range**	**Total counts**	**Model**	τ_1 I_1	τ_2 I_2	τ_3 I_3
	50 ns	3.4 M	3-exp	0.18 ns, 56 %	0.42 ns 42%	21 ns 1.8 %
	Trapping model with thermalization τ_{bulk} = 0.18 ns (fixed)			τ_v=0.22 ns κ_v = 6.5 ns^{-1}	τ_s = 0.47 ns κ_s = 4 ns^{-1}	P_{Ps} = **1 %**, l = 200 nm $\mu = 1.2 \cdot 10^{-4}$, $m/M = 2 \cdot 10^{-6}$
	CDB gaussians (FWHMs, intensities)			4±8 meV, **1%**	15 eV, 93%	69 eV, 5% 306 eV, 0.3%
γ-Al_2O_3 ⌀ 3 μm	**TAC range**	**Total counts**	**Model**	τ_1 I_1	τ_2 I_2	—
	50 ns	3.3 M	2-exp	0.18 ns 97 %	0.95 ns 3 %	
	Trapping model with thermalization τ_{bulk} = 0.18 ns (fixed)			—	0.73 ns κ = 0.17 ns^{-1}	P_{Ps} = 0, l = 900 nm
	CDB gaussians (FWHMs, intensities)			—	18 eV, 97%	97 eV, 3% 303 eV, 0.1%

The initial kinetic energy of positronium atom ejected from the bulk of crystallites was varied manually. We tried values of 1, 2 and 3 eV. It turned out that the value 2 eV leads to the most reasonable agreement with experimental data. The mass ratio m/M was also varied in a similar manner. The obtained value turned out to be $2 \cdot 10^{-6}$. This corresponds to an amount of 20 Al_2O_3 molecules that accept the recoil kinetic energy during collision of a Ps atom with a crystallite.

RESULTS AND DISCUSSION

Fit results of LT and CDB spectra of Al_2O_3 powders of different sizes are given in Table. 1. Spectra were fitted with the model described above (labeled "Trapping model + thermalization") and with the regular 3-exponential model.

Lifetime spectrum of a 3 μm γ-Al_2O_3 powder turns out to be almost mono-exponential. Its crystallites are apparently defect-free crystals, so the e^+ lifetime τ_b = 0.18 ns can be naturally identified with the e^+ bulk lifetime in a defect-free Al_2O_3 crystal (our measurements show, this time is the same for α- and γ-phases).

Individual 3-exponential fits of the spectra of 50 nm and 100 nm powders measured at different recording intervals (50, 100 and 200 ns), do not provide consistent values of the lifetimes τ_1, τ_2 and τ_3 and intensities I_1, I_2 and I_3. Inconsistency is dramatically notable for the longer-living component τ_3 (highlighted in red color in Table 1). However, when application of the two-state trapping model with Ps thermalization, gives consistent results for fitting parameters τ_b, τ_v, τ_s, κ_v, κ_s, m/M and μ. Parameter P_{Ps} – probability of the Ps formation – was fixed to the intensity of the "narrow" component of the CDB spectrum (underlined in the Table 1).

Intensity of the "narrow" component of the CDB spectrum decreases with increase of the crystallite size. We explain this effect as follows. Ps atom (to be more precise, qf-Ps) is formed in a bulk of a crystallite where thermalized e^+ picks up one of the electrons knocked out by energized e^+ during its ionization slowing down. Then qf-Ps diffuses to its surface and escapes the grain into inter-crystallite space. In coarse powders, qf-Ps does not have enough time to reach the crystallite boundary and annihilates in the bulk. For the sake of simplicity in this work we did not take into account formation of qf-Ps and its diffusion to the surface. We do plan to include this effect in the model later on.

We believe that positron states with lifetimes of about 0.26 ns and 0.5 ns in γ-Al_2O_3 correspond to a positron trapped in Al-vacancy and in surf-e^+ state bound on the crystallite surface.

For α-Al_2O_3 powders the intensity of a positron state wit lifetime about 0.5 ns is notably larger compared to γ-Al_2O_3. Technically along with the surface-bound e^+ state there might be some other intergrain e^+ state with the similar lifetime. In fact, this amount of positrons physically cannot reach the surface of crystallite for such a coarse grain powder. This question needs further investigation.

It is likely that the parameter μ characterizes efficiency of Ps ortho-para conversion with collision of oxygen, may correlate with the sorption of O_2 on the surface of crystallites. Our data seemingly indicate that the density of filling the surface with oxygen increases with the enlargement of powder particles.

REFERENCES

[1] Y.Sang, H.Qin, H.Liu et al. J. Eur. Ceramic Soc., V.33(13-14), P. 2617-2623 (2013) https://doi.org/10.1016/j.jeurceramsoc.2013.04.009

[2] C. Dauwe, T. Van Hoecke, D. Segers "Positronium Physics in fine powders of insulating oxides", Proceedings of XXX Zakopane School of Physics "Condensed Matter Studies by Nuclear Methods", Eds. K. Tomala and E.A. Gorlich, Zakopane, Poland, 6-13.05.1995

[3] P.Stepanov et al., paper in this issue

[4] B.Bergersen, M.Stott Solid State Commun., V.7, P. 1203 (1969)

[5] P.S. Stepanov, S.V. Stepanov, V.M. Byakov, F.A. Selim "Developing New Routine for Processing Two-Dimensional Coincidence Doppler Energy Spectra and Evaluation of Electron Subsystem Properties in Metals" Acta Physica Polonica A, Vol. 132(5), pp. 1628-1633 (2017) DOI:10.12693/APhysPolA.132.1628